

Title	Analysis of a Nonlinear Hyperbolic Equation by Energy Method (Discretization Methods and Numerical Algorithms for Differential Equations)
Author(s)	Shimoji, Sadao
Citation	数理解析研究所講究録 (2002), 1265: 18-27
Issue Date	2002-05
URL	http://hdl.handle.net/2433/42069
Right	
Type	Departmental Bulletin Paper
Textversion	publisher

Analysis of a Nonlinear Hyperbolic Equation by Energy Method

下地貞夫

Sadao Shimoji

東京工科大学

Tokyo Engineering University

shimoji@cc.teu.ac.jp

Abstract. We study a nonlinear hyperbolic equation in one dimension, which is derived from the model for a nonlinear lattice, by the viscosity method. We solved the viscosity equation numerically by the central difference scheme. For $0.02 \lesssim \epsilon \lesssim 0.001$, where ϵ is the coefficient of viscosity, the solutions behave as shock waves. For $0 \leq \epsilon \lesssim 0.001$, the solutions oscillate violently, whereas the sum of the mechanical energy and the dissipated energy is conserved. We solved also the original equation by the Godunov's scheme. The solutions are quite similar to those of the viscosity equation for $0.02 \lesssim \epsilon \lesssim 0.001$, but the variation of the dissipated energy with time is not and is complex.

1. Introduction

We consider first a simple one dimensional lattice where the particles interact with the potential proportional to the power of $\gamma + 1$ ($\gamma > 1$) and with no linear term. Then the Hamiltonian $\mathcal{H}_{N,\gamma}$ for the motion is written as;

$$\mathcal{H}_{N,\gamma} = \sum_{i=0}^N \left[\frac{1}{2} \left(\frac{dU_i}{dt} \right)^2 + \frac{1}{\gamma(\gamma+1)a^{\gamma+1}} |U_{i+1} - U_i|^{\gamma-1} (U_{i+1} - U_i)^2 \right], \quad (1)$$

$$U_0 = U_{N+1} = 0,$$

where N is the number of particles in the lattice, a is the lattice constant, U_i is the displacement of the i -th particle from its equilibrium position and t is time.

Interesting results related with this system have been reported : H. Yoshida [1] and K. Umeno [2] showed that the equation of motion from (1) has not any first integral other than the Hamiltonian when the exponent $\gamma + 1$ is the even integer larger than four and the number of particles is odd, and T. Kawai *et al* [3] showed that, by the numerical study, the fluctuation of the phonon number obeys the $1/f$ law and the trajectories of particles spend equal time in all small spheres whose centers are located on the energy surface in the $2n$ dimensional phase space.

However the feature of the collective motion of particle, such as wave motion, in the system is not known in detail, we investigate it in this study.

Considering the case where the number of particles is large, we approximate the displacements $U_i(t)$'s of particles in the semi-discrete system (1) by a continuous distribution

$U(x, t)$, $x = ai$. Then its time development is expressed by a partial differential equation as,

$$U(x, t)_t = |U_x(x, t)|^{\gamma-1} U(x, t)_{xx}. \quad (2)$$

Furthermore putting $u = U_x$ and $v = U_t$, we can express (2) by a pair of conservation laws,

$$u_t - v_x = 0, \quad (3)$$

$$v_t - |u|^{\gamma-1} u_x = 0, \quad 1 < \gamma < \infty. \quad (4)$$

The equations of the form $U_{tt} = (\phi(U)U_x)_x$ have been studied extensively in the field of fluid dynamics, especially on their symmetries [4, 5]. But here we regard Eq. (2) and the system (3, 4) as a model of a nonlinear lattice. That is, it will be treated as dynamically isolated system.

2. The viscosity equation

For a smooth distribution of U_i , the smooth solution of E. (2) and hence the system (3, 4) give a good approximation. But since the system (3, 4) is hyperbolic, its solution becomes discontinuous after a time for a smooth initial data [6]. The equation of motion from (1) is not monotone, it gives an oscillating solution for this discontinuous solution.

The system (3, 4) admits the conservation of total energy, so that its solution can be approximated by the continuous solution of the following viscosity equation,

$$u_t - v_x = \epsilon u_{xx}, \quad (5)$$

$$v_t - |u|^{\gamma-1} u_x = \epsilon v_{xx}, \quad 1 < \gamma < \infty. \quad (6)$$

Here ϵ is the viscosity coefficient. We will investigate the behavior of the continuous solutions of the system (5, 6) and, as a results, the behavior of the discontinuous solutions of the system (3, 4) and so those of Eq. (2).

We consider an initial and boundary value problem of the system (5, 6) with the data,

$$\left. \begin{aligned} u(x, 0) &= u_0(x), \quad v(x, 0) = v_0(x), \\ u(\pm\infty, t) &= u_t(\pm\infty, t) = 0, \\ v(\pm\infty, t) &= v_t(\pm\infty, t) = 0, \end{aligned} \right\} \quad (7)$$

where we assume that $u_0(x)$ and $v_0(x)$ are smooth, and also $u_0, v_0 \in L_2(\mathbf{R}) \cap L_\gamma(\mathbf{R})$. Then we have obtained the following theorem [7].

Theorem. the system (5, 6) has a global solution for the initial boundary value problem with the data (7). The solution decays uniformly to 0 for $x \in \mathbf{R}$ as $t \rightarrow \infty$.

Kanel [8] and Smoller [9] showed the existence of a global solution and its uniform decay over a finite region $x_1 \leq x \leq x_2$ for the gradient system, and the uniform decay of a solution does not hold for the antigradient system with the negative exponent $\gamma < 0$. We have proved our theorem by modifying their method.

3. Numerical analysis of wave form and energy conservation

Taking the value of the exponent of the potential as $\gamma = 3$, we analyze numerically the viscosity equation (5, 6).

We give the initial data as

$$u(x, 0) = \begin{cases} x + 1 & \text{for } -1 \leq x \leq 0, \\ -x + 1 & \text{for } 0 \leq x \leq 1, \\ 0 & \text{for } |x| > 1, \end{cases} \quad (8)$$

$$v(x, 0) = -\frac{1}{2}u(x, 0)^2, \quad (9)$$

$$U(x, 0) = \int_{-\infty}^0 u(x, 0)dx. \quad (10)$$

The system (3, 4) has the Riemann invariants $v \pm u^2/2$, so the solution shows simpler behavior for these data than for the others. The data $u(x, 0)$ and $v(x, 0)$ are not smooth at $|x| = 1, 0$, but the above theorem holds, because they have compact support.

We discretized the system (5, 6) by the central difference scheme, and the numerical integration was performed with $\Delta x = 0.01$ and $\Delta t = 0.0002$.

The results are summarized as :

- (i) for $\epsilon \lesssim 0.001$, the numerical solution oscillated with x ,
- (ii) for $0.001 \lesssim \epsilon \lesssim 0.02$, " the approximate solution of (3, 4) " was obtained,
- (iii) for $\epsilon \gtrsim 0.001$, the numerical solution behaved as a progressing wave.

The central difference scheme is not monotone, and so the solution begins to oscillate about the point where its slope is large for a small value of ϵ as in the case of (i). The linear term is superior to the nonlinear term in the case of (iii). Case (iii) will be discarded.

In our previous work [7], we analyzed the equation numerically with the data $u(x, 0) = e^{-x^2}$ and the relations as Eqs. (9) and (10). The values of the parameters are the same as the present analysis. Although the classical solutions in the previous analysis and those in the present one are different, the solutions corresponding to the discontinuous solutions of the system (3, 4) in the previous analysis and those in the present one are very similar. They approach asymptotically to the identical solutions as time elapses.

3.1. The results of case (ii)

The x -distributions of $u(x, t)$ for $\epsilon = 0.002$ at $t = 0, 2, 4, 6, 8, 10$ are shown in Figure 1. Since the system (3, 4) expresses a wave motion, the points on the solution proceed with t in the right direction of x under the given initial values. The speed of the propagation of a point is proportional to the value of $u(x, t)$. It is greater for the greater value of $u(x, t)$ and the wave form leans to right more and more with time. The slope diverges to infinity at $t = 1.0$, $x = 1.0$. After that time, the solution becomes a weak solution with the

property of a shock. The shock goes to right indefinitely with its decreasing height. The numerical solution of (5, 6) shows this tendency. The maximum of $u(x, t)$, say $u_m(x, t)$, appears about the right end of the wave and the value of $u(x, t)$ decreases rapidly on its right side. The location of $u_m(x, t)$ goes to right and its height decreases with time.

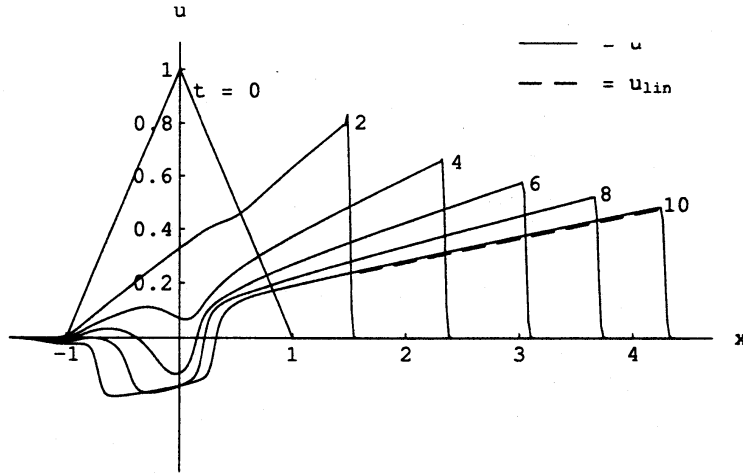


Figure 1. The wave forms for fixed values of t and a linear approximation at $t = 10$.

A dip going to left direction and growing to negative values of $u(x, t)$ is observed. The cause of production of this second wave can be attributable to the interaction of a shock wave and a rarefaction wave, but the detailed discussion is omitted in this study.

In Figure 2, we show the x -distribution of the viscosity term $\epsilon u_{xx}(x, t)$. The distribution has a large value in a narrow region about $u_m(x, t)$ and is zero outside this region. That is, the dissipation of the mechanical energy occurs in this narrow region.

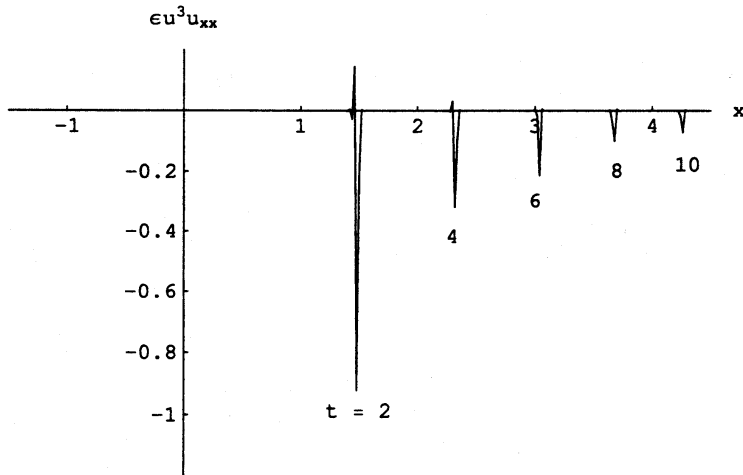


Figure 2. Variation of the distribution of the viscosity term with t .

In Figure 3, we show the characteristic curves which have started from various points on the x -axis at $t = 0$. These curves are obtained by integrating numerically $\frac{dx}{dt} = u(x, t)$ where the numerical solution $u(x, t)$ in Figure 1 is used. It is observed that the characteristics going to right form a single curve and those going to left also form another curve. We will designate the former one as $x(t)$.

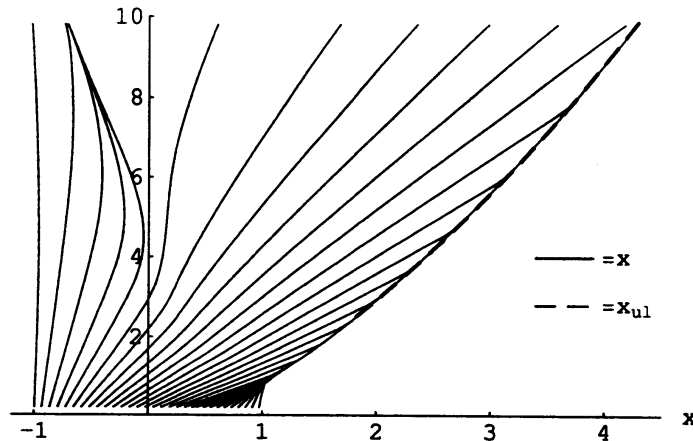


Figure 3. Characteristics of $u(x, t)$ and an approximate shock curve $x_{ul}(t)$.

The curve $x(t)$ expresses the trajectory of $u_m(x, t)$. We show that $x(t)$ expresses the shock curve of the system (3, 4).

Let the position of the discontinuity of the weak solution of (3, 4) be $x = y(t)$, the values on its left side (u_l, v_l), those on the right side (0, 0). Then, the Rankine-Hugoniot jump condition is written as

$$u_l \frac{dy}{dt} = v_l, \quad v_l \frac{dy}{dt} = \frac{1}{3} u_l^3. \quad (11)$$

To relate $x(t)$ and $u_m(x, t)$ with Eq. (11), we approximate $u(x, t)$ in a region left to $u_m(x, t)$ by a linear function,

$$u(x, t) \approx u_{lin}(x, t) = A \frac{x + a}{t + b}, \quad (12)$$

where A , a and b are constants. Using u_{lin} and denoting x_{ul} instead of y , we obtain from Eq. (11)

$$\frac{dx_{ul}}{dt} = \frac{1}{\sqrt{3}} u_{lin} = \frac{A}{\sqrt{3}} \frac{x_{ul} + a}{t + b} \rightarrow x_{ul}(t) = c[(t + b)]^{A/\sqrt{3}} - a. \quad (13)$$

We determine the constants from the values of $u(x, t)$ at $(x, t) = (1.5, 10)$, $(4, 10)$ and those of $x(t)$ at $t = 2, 10$ as $A = 1.0082$, $a = 1.0823$, $b = 1.208$ and $c = 1.2937$. Thus determined u_{lin} and $x_{ul}(t)$ are shown by the dashed lines respectively in Figure 1 and Figure 3. The agreement of u_{lin} with $u(x, 10)$ shows that the approximation to $u(x, t)$ by a linear function u_{lin} is good. And the agreement of $x_{ul}(t)$ with $x(t)$ means that the curve $x(t)$ satisfies the jump condition for the system (3, 4). Consequently, the solution of the system (5, 6) for this case can be said to approximate that of (3, 4).

3.2. The results of case (i)

In case (i), the numerical solution oscillate around its maximum. So the collective motion will be observed better by the integral $U(x, t) = \int_{-\infty}^x u(x, t) dx$ rather than by $u(x, t)$. For

$\epsilon = 0.0$, we discretize Eq. (2) for $\gamma = 3$ as,

$$U_i^{k+1} = U_i^k \Delta t + v_i^k, \quad (14)$$

$$v_i^{k+1} = v_i^k \Delta t + \frac{1}{3(\Delta x)^4} ((U_{i+1}^k - U_i^k)^3 - (U_i^k - U_{i-1}^k)^3), \quad (15)$$

where U_i^k and v_i^k are the average values of respectively $U(x, t)$ and $v(x, t)$ in the "cell" $[(i - \frac{1}{2})\Delta x]$ at $t = k\Delta t$. It can be seen that Eqs. (14) and (15) conserve the discretized form of the Hamiltonian (1) for $\gamma = 3$

$$\mathcal{H}_{N,3} = \sum_{i=1}^N = \left\{ \frac{1}{2}(v_i^k)^2 + \frac{1}{12(\Delta x)^4} [(U_{i+1}^k)^4 - (U_{i-1}^k)^4] \right\} \quad (16)$$

with respect to t . We give the initial values as Eqs. (9) and (10). The values $\Delta x = 0.01$ and $\Delta t = 0.0002$ are also used.

The distribution of $U(x, t)$ with x at $t = 0, 2, 4, 6, 8, 10$ are shown in Figure 4.

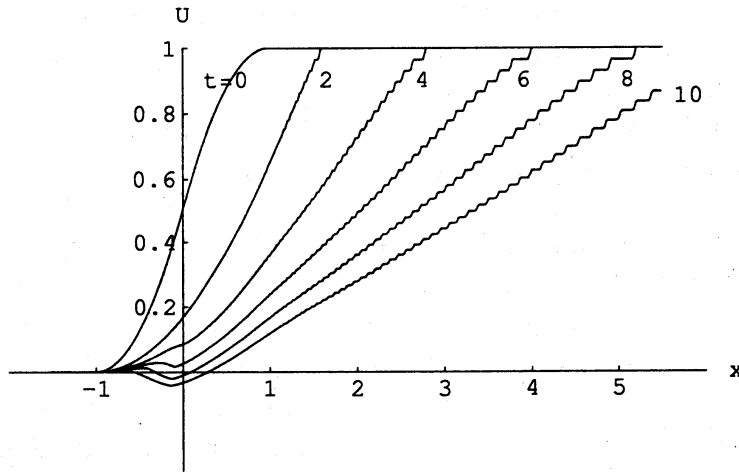


Figure 4. The integral curve at each time, $\epsilon = 0$.

It is observed that $U(x, t)$ at each t increases with x and arrives at the value of $U(x, 0)$ at a point, say $x = x_0(t)$. Then, it remains constant. This means that the integral of $u(x, t)$ in the whole region of x , $U(\infty, t) = \int_{-\infty}^{\infty} u(x, t) dx = U(\infty, 0)$, is independent of t and conserved. A dip glowing to left is also observed.

For $0 < \epsilon \lesssim 0.001$, we obtained $U(x, t; \epsilon)$ by integrating the oscillating numerical solution of the system (5, 6) with respect to x . The behavior of $U(x, t; \epsilon)$ is similar to that of $U(x, t)$ shown in Figure 4, but the dip going left is larger.

Let the point where the value of $U(x, t; \epsilon)$ arrives at that of $U(x, 0)$ be x_ϵ . Then x_ϵ locates the right end of the region where the motion diffuses until the time t . The curve designated as x_{U_0} for $\epsilon = 0.0$, x_{u_1} for $\epsilon = 2 * 10^{-5}$ and x_{U_2} for $\epsilon = 2 * 10^{-4}$ are shown in Figure 5. We observe that $x_\epsilon(t)$ increases faster, namely the speed of diffusion of motion is faster, for the smaller value of ϵ . The curve $x = x_\epsilon(t)$ for $\epsilon = 0.0002$ must be close to that of $x = x(t)$ shown in Figure 3.

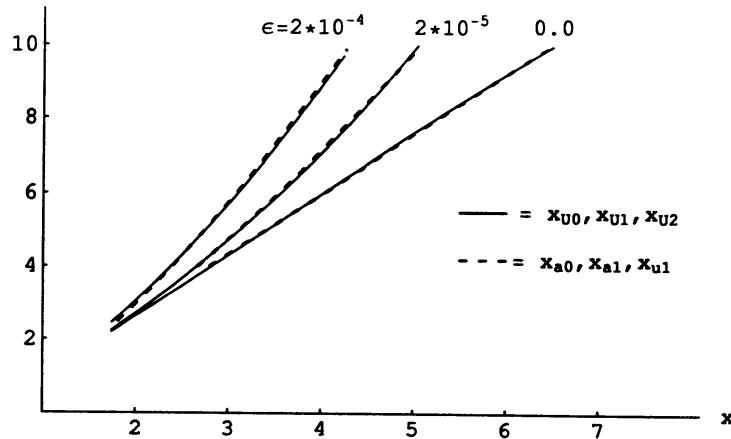


Figure 5. The movement of the head for each value of ϵ .

To see the variation of $x_\epsilon(t)$ with ϵ precisely, we approximate $x_\epsilon(t)$ by a function similar to that in Eq. 13, $x_{a,\epsilon}(t) = c[(t+b)]^{A_1} - a$. For $\epsilon \lesssim 0.0002$ the numerical solutions of $u(x,t) = U_x(x,t)$ oscillate violently with x and the jump condition is not applicable. So we use $x_{a,\epsilon}$ to express the speed of diffusion of motion with no relation to this condition. The constants are chosen as $(A_1, a, b, c) = (0.6811, 0.6873, 0.8506, 1.1223)$ for $\epsilon = 0.00002$ and $(1, 0.020, 0.5806, 0.615)$ for $\epsilon = 0.0$. The corresponding functions are designated respectively as $x_{a,0}$ and $x_{a,1}$. They are plotted with the dashed lines in Figure 5. There is also plotted x_{ul} in case (ii). It agrees with $x_\epsilon(t)$ for $\epsilon = 2 * 10^{-4}$. This shows that the variation of $x_\epsilon(t)$ with ϵ is small for $\epsilon = 0.002 \sim 0.0002$. The value of A_1 which expresses the speed of the diffusion of motion increases up to $A_1 = 1$ with the decrease of ϵ .

For $\gamma = 3$, the speed of diffusion of motion by the system (5, 6) for $\epsilon = 0.002$ and so that of the system (3, 4) are estimated to be proportional to $t^{A/\sqrt{3}} = t^{0.5821}$. The speed for $\epsilon = 0.0$, that is in the lattice with Eq. (1), is larger and is proportional to t . The value of $A_1 = 1$ is compared to that predicted theoretically for weak shocks [5].

3.3. Energy conservation

We show the variations of various types of energy with t in Figure 6 where the mechanical energy, the dissipated energy and the total energy are plotted. The mechanical energy, which is the sum of potential energy E_u and the kinetic energy E_v ;

$$E_u = \int_{-\infty}^{\infty} \frac{1}{12} u(x,t)^4 dx, \quad E_v = \int_{-\infty}^{\infty} \frac{1}{2} v(x,t)^2 dx,$$

is designated as E_{m1} and E_{m2} respectively for $\epsilon = 2 * 10^{-5}$ and $2 * 10^{-3}$. The dissipated energy, which is the sum of E_{uv} dissipated from E_u and E_{vv} dissipated from E_v by the effect of the "viscosity";

$$E_{vu} = -\epsilon \int_0^t \int_{-\infty}^{\infty} u^3 u_{xx} dx dt, \quad E_{vv} = -\epsilon \int_0^t \int_{-\infty}^{\infty} v v_{xx} dx dt,$$

is designated as E_{d1} and E_{d2} respectively for $\epsilon = 1 * 10^{-5}$ and $2 * 10^{-3}$. The total energy is the sum $E_i = E_{mi} + E_{di}$, $i = 1, 2$. For $\epsilon = 0.0$ the amount of the dissipated energy is

zero and so the total energy is the same as the mechanical energy.

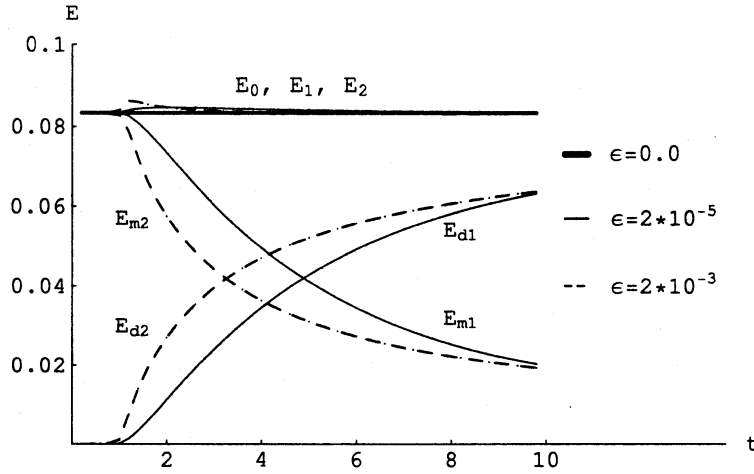


Figure 6. Variation of each kind of energy with time.

It is observed that the mechanical energy decreases and the dissipated energy increases with time. The decrease of E_{m2} is faster than that of E_{m1} initially, but they come close to each other as time goes on.

The total energy is seen to be conserved for all the values of ϵ shown in Figure 6.

4. Solutions of conservation laws (3, 4) by Godunov's method

To assure that we have obtained the approximate solutions of the system (3, 4) in case (ii), we solve the system (3, 4) by the Godunov's upwind scheme with the Roe-Pike's approximate Riemann solver.

The Roe-Pike's linearized equation for our system is

$$\mathbf{u}_t + \mathbf{A}\mathbf{u}_x = \begin{pmatrix} u \\ v \end{pmatrix}_t + \begin{pmatrix} 0 & -1 \\ -u_m^2 & 0 \end{pmatrix} \begin{pmatrix} u \\ v \end{pmatrix}_x = 0, \quad (17)$$

where

$$u_m = \sqrt{\frac{u_i^2 + u_i u_{i+1} + u_{i+1}^2}{3}}. \quad (18)$$

We solve the Riemann problem of Eq. (17) with Eq. (18) for the initial data,

$$\mathbf{u}(x) = \mathbf{u}_i, \quad x < 0 \quad \text{and} \quad \mathbf{u}(x) = \mathbf{u}_{i+1}, \quad x > 0. \quad (19)$$

The solution is,

$$\mathbf{u}_{i+\frac{1}{2}}(0) = \frac{1}{2} \begin{pmatrix} u_i + u_{i+1} \\ v_i + v_{i+1} \end{pmatrix} + \frac{1}{2} \begin{pmatrix} (v_{i+1} - v_i)/u_m \\ u_m(u_{i+1} - u_i) \end{pmatrix},$$

where $\mathbf{u}(0)$ is written as $\mathbf{u}_{i+\frac{1}{2}}(0)$. Then the Godunov flux $\mathbf{F}_{i+\frac{1}{2}}(0)$ is given by,

$$\mathbf{F}_{i+\frac{1}{2}}(0) = \mathbf{A}\mathbf{u}_{i+\frac{1}{2}}(0) = -\frac{1}{2} \begin{pmatrix} v_i + v_{i+1} \\ u_m^2(u_i + u_{i+1}) \end{pmatrix} - \frac{u_m}{2} \begin{pmatrix} u_{i+1} - u_i \\ v_{i+1} - v_i \end{pmatrix}. \quad (20)$$

Similarly obtaining $F_{i-\frac{1}{2}}(0)$, we calculate the development of u with time in the form

$$u_i(\Delta t) = u_i(0) + \frac{\Delta t}{\Delta x} [F_{i-\frac{1}{2}}(0) - F_{i+\frac{1}{2}}(0)]. \quad (21)$$

The values of $\Delta x = 0.005$ and $\Delta t = 0.0004$ are used.

The solutions at $t = 0, 2, 4, 6, 8, 10$ are shown in Figure 7. These solutions and those obtained in case (ii) in the preceding section are quite similar. The linear function u_{lin} with the same values of the parameters in case (ii) is plotted by a dashed line and is observed to approximate the solution $u(x, 10)$ in Figure 7 very well.

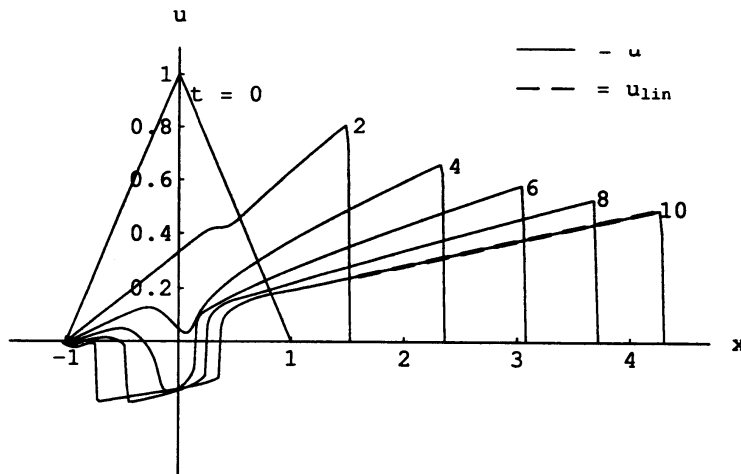


Figure 7. The development of the wave form with time by the upwind method.

The variation of mechanical energy E_m with t is shown in Figure 8, where the variation of "dissipated energy" $E_d = \epsilon_G u_{xx}(t)$, where $\epsilon_G = 0.001$, with t and that of the sum $E = E_m + E_d$ are also shown.

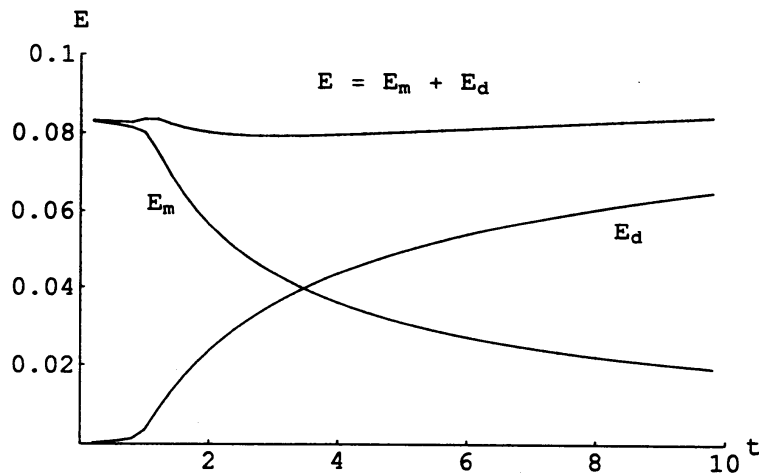


Figure 8. Variation of each kind of energy with time by the upwind method.

The sum $E = E_m + E_d$ is not said to be kept constant with t . This means that the dissipation mechanism involved in the Godunov's scheme is more complex than that is expressed by the simple model of $E_d = \epsilon_G u_{xx}(t)$ with a constant value of ϵ_G .

References

- [1] H. Yoshida, A criterion for the non-existence of an additional Integral in Hamiltonian systems with a homogeneous potential, *Physica*, **29D** (1987) 128-142.
- [2] K. Umeno, Galois extensions in Kowalevski exponents and nonintegrability of non-linear lattices, *Phys. Lett.*, **A190** (1994) 85-89.
- [3] T. Kawai, T. Kobayashi and S. Morita, Lattice dynamics with x^4 potential, Proc. 6th Joint EPS-APS Int'l Conf. on Physics Computing, Lugano Switzerland (1994) 433.
- [4] W. F. Ames, R. J. Postel and E. Adams, Group properties of $u_{tt} = [f(u)u_x]_x$, *Int. J. Nonlinear Mech.*, **16(5-6)** (1981) 439.
- [5] N. H. Ibragimov: CRC Handbook of Lie Group Analysis of Differential Equations, Vol. 1 (1995) CRC Press, Inc.
- [6] P. Lax, Hyperbolic Systems of Conservation Laws and the Mathematical Theory of Shock Waves, *Conf. Board Math Sci.*, **11**, SIAM, 1973.
- [7] S. Shimoji, Proc. 2001 DCDIS Conf., to appear.
- [8] Y. Kanel: Zh. Vychislit. Matem. i Matem. Fiziki, **6** (1966) 466; English transl. in USSR Comp. and Math. Physics, **6** (1966) 74.
- [9] J. Smoller: Shock Waves and Reaction-Diffusion Equations, Springer-Verlag, 1994.